

Magnetic moments of the $\frac{3}{2}^-$ and $\frac{5}{2}^-$ states in $^{107,109}\text{Ag}$

D. Ballon,* Y. Niv,[†] S. Vajda,[‡] N. Benczer-Koller, and L. Zamick
Department of Physics, Rutgers University, New Brunswick, New Jersey 08903

G. A. Leander

UNISOR, Oak Ridge Associated Universities, Oak Ridge, Tennessee 37830

(Received 2 October 1985)

The ratios of g factors of the first excited states of the $^{107,109}\text{Ag}$ isotopes, $g(\frac{3}{2}^-)/g(\frac{5}{2}^-)=1.5(3)$ and $2.3(5)$, respectively, have been measured by the perturbed angular correlation transient field technique. The absolute magnitudes of the g factors have been obtained through a calibration procedure that makes use of the magnetic dipole moments of the first 2^+ states of ^{106}Pd and ^{110}Cd and are ^{107}Ag : $g(\frac{3}{2}^-)=0.61(12)$, $g(\frac{5}{2}^-)=0.41(7)$ and ^{109}Ag : $g(\frac{3}{2}^-)=0.66(10)$, $g(\frac{5}{2}^-)=0.29(6)$. These results are compared with weak coupling calculations as well as with Nilsson models with symmetric or triaxial cores. The latter reveal a sensitive dependence of the g factors on the deformation parameter γ .

I. INTRODUCTION

Precision measurements¹ of magnetic moments of low lying states of even-even nuclei in the vibrational region have amply confirmed the predictions² of the interacting boson approximation model (IBA-2). The model has been extended to the study of odd nuclei by considering the effect of the odd fermion coupled to the underlying boson structure (IBFM).³ However, few critical tests of the model, such as provided by magnetic moment measurements, exist for odd A nuclei. The structure of odd isotopes had originally been examined in the framework of the "weak-coupling" model of de Shalit.⁴ In the simplest characterization, the states of the odd nucleus arise from the coupling of an odd nucleon in its lowest single particle state to either the ground state or the excited states of the even-even core. This approach has had however very limited success and it soon became clear that a mixing of several of the lowest configurations of the odd particle is necessary to account for the observed structure.^{5,6} Furthermore, it is well known that the first excited 2^+ states of the $^{106,108}\text{Pd}$ isotopes exhibit large quadrupole moments in spite of their apparent vibrational structure.⁷ Thus, a calculation of the coupling of the odd proton to a deformed core is a model that might be tested in the description of the structure of the $^{107,109}\text{Ag}$ isotopes. The same arguments apply to IBA calculations, where the symmetry scheme that applies to even-even nuclei is broken by the coupling with the odd particle in its mixed configuration state.

The method of transient hyperfine magnetic fields has been extended to these nuclei in order to determine magnetic moments of the low lying $\frac{3}{2}^-$ and $\frac{5}{2}^-$ states with greater precision than obtained in earlier recoil-in-gas measurements. However, the transient field at Ag ions cannot be calibrated absolutely because there is no Ag isotope with a state whose magnetic moment is known from direct methods (Mössbauer effect or perturbed angular

correlations in an external field, for example) and which can also be examined via the transient field technique. Thus only ratios of magnetic moments can be unambiguously obtained. Nevertheless, to the extent that the transient field in Ag can be approximated by the field in nuclei of adjacent atomic number, an adequate calibration of the field can be obtained by interpolating the results from previous measurements on the neighboring isotopes ^{106}Pd and ^{110}Cd . As a check on the technique and on the calibration, and because Pd also happens to form a possible choice for the core of Ag, the magnetic moment of the 2^+ state in ^{108}Pd was remeasured under the experimental conditions similar to those used for the Ag isotopes.

While these experiments were in progress, two other groups reported similar investigations with results in very good agreement with those reported here.^{8,9}

II. EXPERIMENTAL TECHNIQUES

The energy level diagrams of the $^{107,109}\text{Ag}$ isotopes are displayed in Fig. 1 and the relevant spectroscopic data are summarized in Table I.

The details of the experimental technique have been thoroughly described in previous publications¹ and only the details specific to the present experiments will be given here. The measurements were made on triple-layered targets consisting of the isotope of interest, a layer of ferromagnetic iron, and a stopping layer of copper. The composition of individual targets is summarized in Table II.

The $^{107,109}\text{Ag}$ nuclei were Coulomb excited into the first $\frac{3}{2}^-$ and $\frac{5}{2}^-$ excited states by 80 MeV ^{32}S beams from the Rutgers tandem accelerator. The rate of coincidences between backscattered ^{32}S ions counted in an annular surface barrier detector and the decay gamma rays detected in four NaI(Tl) detectors, was recorded. Typical coincidence spectra of ^{107}Ag and ^{108}Pd are shown in Fig. 2. For the precession measurements the four gamma ray

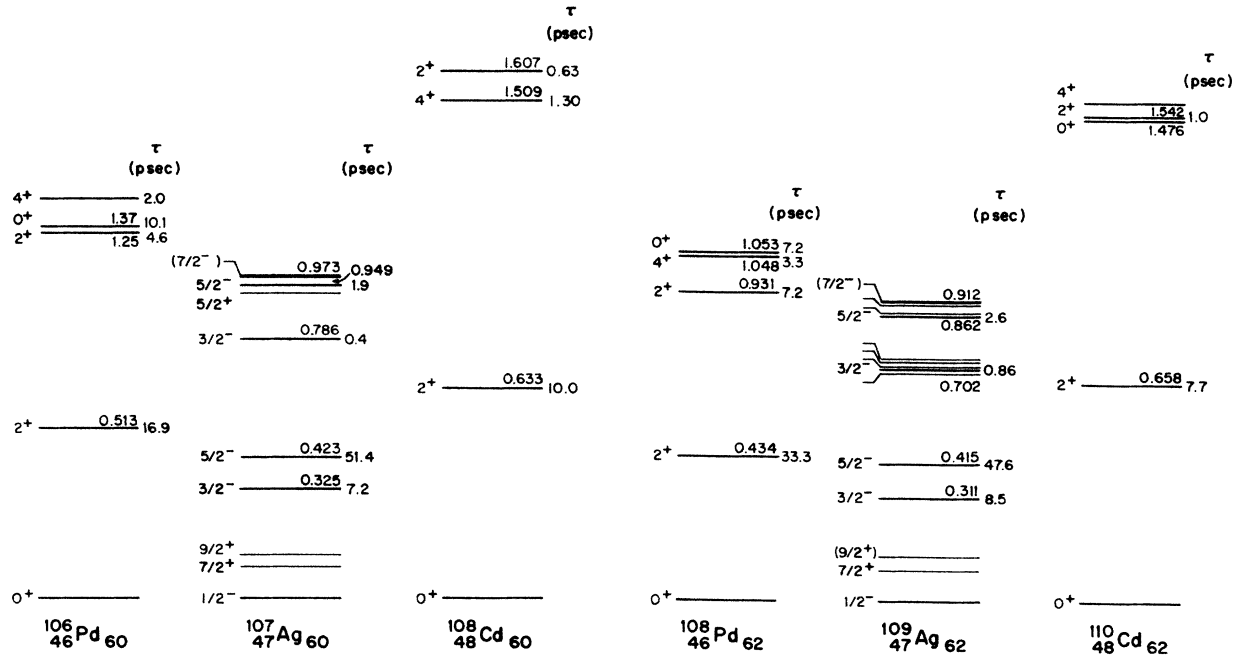


FIG. 1. Energies and lifetimes of the low lying states in the silver and palladium isotopes.

detectors were placed at angles, $\theta = (\pm 55^\circ, \pm 125^\circ)$, $(\pm 65^\circ, \pm 115^\circ)$, or $(\pm 67.5^\circ, \pm 112.5^\circ)$ where the logarithmic slope $S = (1/W)(dW/d\theta)$ of the gamma ray angular correlation $W(\theta)$ is large for the $\frac{3}{2}_1^- \rightarrow \frac{1}{2}_1^-$, $\frac{5}{2}_1^- \rightarrow \frac{1}{2}_1^-$ transitions in the Ag isotopes as well as for the $2_1^+ \rightarrow 0_1^+$ transition in ^{108}Pd .

Angular correlation measurements were carried out for each target several times during the course of the experiment. The data were fitted to the theoretical expressions $W(\theta)$ corresponding to the appropriate transitions. The logarithmic slopes S at the angle where the precession measurements were made were obtained from the fits. A typical particle-gamma angular correlation $W(\theta)$ is shown in Fig. 3 and the resulting parameters are summarized in Table III. An aligning external field of 0.045 T was used to magnetize the iron foils and was reversed every few minutes.

The iron foils were annealed at 1073 K for one hour. Their magnetization was measured before and after each run by a double coil induction magnetometer and is given in Table II. The magnetization of the foils remained constant throughout the experiment.

III. ANALYSIS AND RESULTS

The net precession of the gamma ray angular distribution under reversal of the external magnetic field was obtained from the ratio

$$\rho_{ij} = [(N_i^{\uparrow}/N_i^{\downarrow}) / (N_j^{\uparrow}/N_j^{\downarrow})]^{1/2}.$$

The subscripts $i = 1, 2, j = 3, 4$ represent the four detectors, $N_{ij}(\uparrow, \downarrow)$ is the random- and background-subtracted field up or down coincidence counting rate in the photopeak of the i th or j th detector. The rotation $\Delta\theta$ of the an-

gular distribution was obtained from the measured effect

$$\epsilon = (\rho - 1) / (\rho + 1),$$

where

$$\rho = (\rho_{14} / \rho_{23})^{1/2}.$$

The cross ratios

$$\rho_c = (\rho_{24} / \rho_{13})^{1/2}$$

which should be unity if there are no instrumental asymmetries were continuously monitored.

The analysis of the photopeak is straightforward in the case of the $2_1^+ \rightarrow 0_1^+$ and $\frac{5}{2}_1^- \rightarrow \frac{1}{2}_1^-$ transitions in ^{108}Pd and the Ag isotopes, respectively. The photopeaks of the $\frac{3}{2}_1^- \rightarrow \frac{1}{2}_1^-$ transitions in $^{107,109}\text{Ag}$, on the other hand, consist of three contributions: direct excitation, cascade decay from the $\frac{5}{2}_1^-$ state which is excited simultaneously with the $\frac{3}{2}_1^-$ state, and a Compton background corresponding to the Compton distribution from the $\frac{5}{2}_1^- \rightarrow \frac{1}{2}_1^-$ photopeak.

The measured angular shift $\Delta\theta_{\text{meas}}$ is given by:

$$\Delta\theta_{\text{meas}} = \epsilon_{\text{meas}} / S_{\text{meas}},$$

where

$$\epsilon_{\text{meas}} = \sum \epsilon_i N_i / \sum N_i$$

and

$$S_{\text{meas}} = \sum S_i N_i / \sum N_i$$

and the subscript $i = \text{dir, com, cas}$ stands for direct, Compton background, and cascade contributions, respectively. The ϵ_i are the asymmetries that would be observed

if these contributions to the gamma ray spectrum could be measured separately; the S_i are the corresponding logarithmic slopes of the gamma ray angular distributions. The N_i represent the photopeak intensities summed over both field directions.

The energy of the ^{108}Pd transition corresponds closely to the $\frac{5}{2}_1^- \rightarrow \frac{1}{2}_1^-$ transition in the Ag isotopes. Angular correlation and precession measurements were carried out on the Compton distribution of the ^{108}Pd gamma ray spectrum, yielding $S_{\text{com}} \sim 0$ at angles near 65° , thus implying $\epsilon_{\text{com}} \sim 0$ for these angles. Assuming that similar results would ensue in Ag, the expression for the precession

reduces to:

$$\begin{aligned} \Delta\theta_{\text{meas}} &= (\epsilon_{\text{dir}} + \alpha\epsilon_{\text{cas}}) / (S_{\text{dir}} + \alpha S_{\text{cas}}) \\ &= \Delta\theta_{\text{dir}} / (1 + \alpha S_{\text{cas}} / S_{\text{dir}}) \\ &\quad + \Delta\theta_{\text{cas}} / (1 + S_{\text{dir}} / \alpha S_{\text{cas}}), \end{aligned}$$

where $\Delta\theta_{\text{dir}}$ represents the precession of the moment of the directly excited $\frac{3}{2}_1^-$ state, $\alpha = N_{\text{cas}} / N_{\text{dir}}$, and $\Delta\theta_{\text{cas}} \sim \Delta\theta_{5/2}$ because, since the mean life of the $\frac{5}{2}_1^-$ state is long, the Ag ions created in the $\frac{5}{2}_1^-$ state traverse the iron foil in that state and come to stop in the copper back-

TABLE I. Summary of spectroscopic data and of g -factor measurements in the Ag and neighboring Pd and Cd isotopes.

E (MeV)	$I\pi$	τ (psec)	Technique ^a	Ref.	g	$\frac{g(\frac{3}{2})}{g(\frac{5}{2})}$	Technique ^a	Ref.	Q (e b)	Ref.	
^{107}Ag	$\frac{1}{2}^-$	7.2(13)	RDM	10	-0.227						
					0.325	$\frac{3}{2}^-$	0.51(7) ^b	1.12(29)	RIG	17	
						0.63(9)	1.70(37)	TF	8		
						0.70(10)	1.70(35)	TF	9		
						0.61(12)	1.49(31)	TF	This work		
						1.5(2) ^c	Average				
		$\frac{5}{2}^-$	43.5(29)	RDM	10	0.43(15) ^b		RIG	17		
			54.3(25)	CE	11	0.37(6)		TF	8		
			51.4(24)	RDM	12	0.41(6)		TF	9		
						0.41(7)		TF	This work		
^{109}Ag	$\frac{1}{2}^-$	8.5(10)	RDM	10	-0.261						
					0.311	$\frac{3}{2}^-$	0.56(18) ^b	1.66(33)	RIG	17	-0.54 \rightarrow -0.91 ^d
						0.77(10)	2.14(41)	TF	8		
						0.75(11)	2.14(53)	TF	9		
						0.66(10)	2.30(48)	TF	This work		
						2.1(3) ^c	Average				
		$\frac{5}{2}^-$	50.5(28)	RDM	10	0.33(10) ^b		RIG	17	-0.16 \rightarrow -0.54 ^d	19
			55.8(54)	CE	11	0.36(5)		TF	8		
			47.6(20)	RDM	12	0.35(7)		TF	9		
						0.29(6)		TF	This work		
^{106}Pd	0.513	2^+	16.9(9)	$B(E2)$	13	0.40(2)		RPAC	18	-0.50(5)	20
^{108}Pd	0.434	2^+	33.3(9)	$B(E2)$	14	0.36(3)		TF	16	-0.56(3)	14
^{108}Cd	0.633	2^+	10.0(14)	$B(E2)$	14	0.34(9)		TF	16	-0.45(8)	14
^{110}Cd	0.658	2^+	7.7(6)	$B(E2)$	15	0.29(6)		RPAC	18	-0.40(4)	15

^a Abbreviations in the table stand for the following: RDM is the recoil distance method, CE is the Coulomb excitation, RIG is the recoil in gas, TF is the transient field, RPAC is the radioactivity-perturbed angular correlation.

^b Renormalized to $g(^{110}\text{Pd}, 2^+) = 0.31(3)$, Ref. 16.

^c Average results of this work and of Refs. 8 and 9.

^d A range of acceptable quadrupole moments is given because the sign of the relevant matrix elements was not known.

TABLE II. Summary of target configuration and kinematics of the recoiling ion. l is the thickness of the target isotope. L is the thickness of the iron layer. M is the magnetization of the ferromagnetic layer in an external field $H_{\text{ext}}=0.045$ T.

Isotope	Ref.	Target	l (mg/cm ²)	L (mg/cm ²)	M^a (T)	$E(^{32}\text{S})$ (MeV)	E_{in} (MeV)	E_{out} (MeV)	$(v/v_0)_{\text{in}}$	$(v/v_0)_{\text{out}}$
¹⁰⁷ Ag	This work	I	0.79	1.45	0.1748	80	46.9	19.8	4.2	2.8
	This work	II	0.62	1.51	0.1744	80	48.8	20.1	4.3	2.8
¹⁰⁹ Ag	This work	III	0.53	1.50	0.1754	80	49.3	20.9	4.3	2.8
¹⁰⁸ Pd	This work		0.63	1.55	0.1729	80	48.3	15.0	4.2	2.7
	Ref. 16		0.77	1.33	0.1759	72	43.7	20.4	4.0	2.7
	Ref. 16		0.60	1.35	0.1754	64	40.2	17.9	3.9	2.6

^aThe magnetization of these foils is measured relative to that of the iron samples from which the parametrization of the transient field was obtained and which were fully saturated. The uncertainty in the magnetization measurement is of the order of 3%.

ing before cascading through the $\frac{3}{2}_1^-$ state. Thus,

$$\Delta\theta_{\text{dir}} = \Delta\theta_{\text{meas}} + \alpha(S_{\text{cas}}/S_{\text{dir}})(\Delta\theta_{\text{meas}} - \Delta\theta_{5/2}).$$

The ratio $S_{\text{cas}}/S_{\text{dir}}$ and the intensity parameter α must be calculated. The parameter α is related to the excitation cross sections σ , the branching ratio $B = (\frac{5}{2}_1^- \rightarrow \frac{3}{2}_1^-) / (\frac{5}{2}_1^- \rightarrow \frac{1}{2}_1^-)$, and the angular correlation functions $W(\theta)$ by the expression

$$\alpha(\theta) = B(\sigma_{1/2 \rightarrow 3/2} / \sigma_{1/2 \rightarrow 5/2}) [W_{\text{cas}}(\theta) / W_{\text{dir}}(\theta)].$$

The cross sections were calculated from Coulomb excitation theory to be 0.70 and 0.69 for ¹⁰⁷Ag and ¹⁰⁹Ag, respectively, and the corresponding branching ratios were taken¹¹ as 4.6% and 6.4%. The angular correlation functions were also derived from theory assuming that only

the $\pm\frac{1}{2}$ substates were populated in the backscatter geometry of this experiment and assuming further that the $\pm\frac{1}{2}$ substates of the $\frac{3}{2}_1^-$ state were populated with the same intensity as those of the $\frac{5}{2}_1^-$ state. The latter were in fact determined from the analysis of the $\frac{5}{2}_1^- \rightarrow \frac{1}{2}_1^-$ transition. The multipolarity mixing parameters $\delta(^{107}\text{Ag}) = -0.207$ and $\delta(^{109}\text{Ag}) = -0.193$ were used.¹¹ The relevant slopes were calculated from the resulting angular correlation expressions and the ratios $S_{\text{cas}}(\theta)/S_{\text{d}}(\theta) = 0.41, 0.44,$ and 0.45 at $\theta = 55^\circ, 65^\circ,$ and 67.5° were obtained. The parameters α were 0.03 and 0.04 for ¹⁰⁷Ag and ¹⁰⁹Ag, respectively.

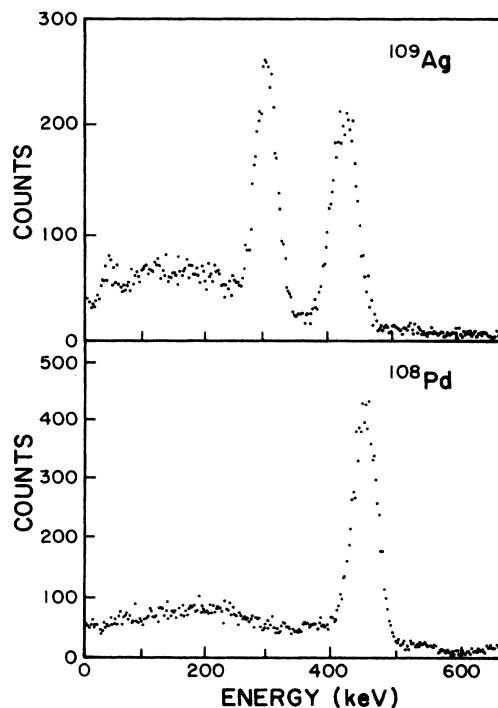


FIG. 2. Typical coincidence gamma-ray spectra for ¹⁰⁹Ag and ¹⁰⁸Pd.

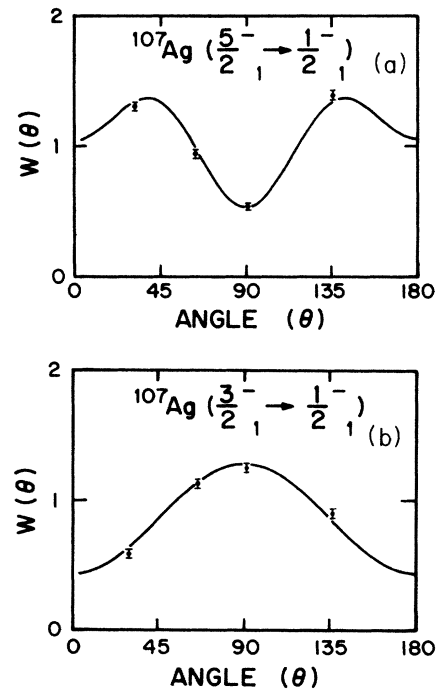


FIG. 3. Measured particle-gamma ray angular correlation functions for (a) the $\frac{1}{2}_1^- \rightarrow \frac{5}{2}_1^- \rightarrow \frac{1}{2}_1^-$ transition and (b) the combination of direct, Compton, and cascade contributions in the $\frac{1}{2}_1^- \rightarrow \frac{3}{2}_1^- \rightarrow \frac{1}{2}_1^-$ transition.

TABLE III. Summary of the logarithmic slopes, experimental precession angles, and the relative g factors, g_r , derived from the data and the transient field parametrization described in the text.

Isotope	Target	θ	S	$\frac{\frac{5}{2}^- \rightarrow \frac{1}{2}^-}{\Delta\theta}$ (mrad)	g_r	S	$\frac{\frac{3}{2}^- \rightarrow \frac{1}{2}^-}{\Delta\theta_{\text{meas}}}$ (mrad)	$\Delta\theta$ (mrad) ^a	g_r
¹⁰⁷ Ag	I	65°	-1.53(3)	-9.4(15)	0.393(63)	0.57(2)	-13.0(30)	-13.1(30)	0.555(130)
	II	67.5°	-1.55(5)	-8.7(17)	0.353(69)	0.55(2)	-13.5(33)	-13.6(33)	0.560(136)
	Average					0.375(47)			0.557(94)
¹⁰⁹ Ag	III	55°	-0.97(2)	-9.2(48)		0.79(2)	-23.4(52)	-23.7(52)	
	III	65°	-1.47(3)			0.61(1)			
	III	65°	-1.47(3)	-6.3(12)		0.60(1)	-13.1(20)	-13.2(20)	
	III	65°	-1.46(4)			0.61(1)			
	III	67.5°	-1.56(3)	<u>-6.0(50)</u>		0.51(4)	-23.3(107)	<u>-23.6(107)</u>	
	Average				-6.5(11)	0.263(45)		-14.8(18)	0.606(74)
¹⁰⁸ Pd		67.5°	-3.00(9)	-5.8(9)	} 0.304(27)	Ref. 16			
		67.5°	-3.11(4)	-7.5(8)					
		67.5°	-3.11(4)	-7.1(7)	0.288(29)	This work			

^a $\Delta\theta_{\text{meas}}$ was corrected as described in the text to incorporate the direct and cascade contributions to the $\frac{3}{2}^- \rightarrow \frac{1}{2}^-$ radiation.

Finally, relative g factors, g_r , were obtained from the measured precessions from calculations of the following expressions:

$$\Delta\theta = \int \delta\theta dN / \int dN$$

and

$$\delta\theta = -g_r(\mu_N/\hbar)B_R(v,Z)dt$$

where dN is the population distribution of the state of interest, and

$$B_R(v,Z) = 96.7(v/v_0)^{0.45}Z^{1.1}M \equiv CB(v,Z).$$

The field B_R corresponds to a parametrization of the transient field derived by the Rutgers group²¹ from measurements on a variety of ions from O to Sm. A scaling factor C normalizes this parametrized field B_R to the actual field $B(v,Z)$ that acts on any specific ion traversing a particular ferromagnetic foil. This scaling factor should be obtained from the measurement of the spin precession of a state whose magnetic moment has been unambiguously measured by independent techniques. No such calibration case exists, however, for Ag ions. The next best procedure that can be used to obtain an absolute calibration of the transient field involves interpolation of calibra-

tions of the field obtained for nearby ions in the same velocity range, in the present case, ¹⁰⁶Pd and ¹¹⁰Cd. Table IV presents the data from which the scaling factors C for Pd and Cd ions traversing iron foils were derived. A scaling factor for Ag ions, $C=1.09(11)$ was interpolated from these data and was used to obtain absolute g factors $g = Cg_r$, displayed in Table I. Note that the errors in these g factors include the statistical error in the precession measurement as well as the error in the scaling factor. The error in the scaling factor, in turn, reflects the statistical fluctuations in the original precession measurement, in the lifetime, and in the transient field calibration run. The ratio of g factors, however, is free from the uncertainties arising from the transient field calibrations, and the average of the ratios obtained in the three transient field experiments was computed (Table I).

The results of this experiment agree fairly well with those of Stuchbery *et al.*⁸ and of Bazzacco *et al.*⁹ which were carried out under fairly different experimental conditions. In the Stuchbery *et al.*⁸ experiments cobalt was used as the ferromagnet. Bazzacco *et al.*⁹ used iron, the Rutgers parametrization B_R , a scaling factor $C=1.20(11)$, and a further normalization factor of 0.94 obtained from measurements on ¹⁰⁶Pd.

TABLE IV. Comparison of the experimental g factors, g_r , in ¹⁰⁶Pd and ¹¹⁰Cd obtained by the transient field technique with the accepted values determined from radioactivity measurements required for the calibration of the transient field for Pd and Cd isotopes.

	g_r^a	Ref.	g^b	Ref.	τ (psec)	Ref.	$C = g/g_r$
¹⁰⁶ Pd	0.348(30)	16	0.40(2)	18	16.9(9)	13	1.14(12)
¹¹⁰ Cd	0.308(44)	16	0.28(6)	18	7.7(6)	15	0.93(22)
Ag	Interpolated value						1.09(11)

^a g_r is obtained from transient field measurements assuming the transient field is given by B_R .

^b g is the value of the g factor obtained from radioactivity, or perturbed angular correlation measurements, and recalculated for the latest measurement of the mean life.

TABLE V. g factors in the single particle model.

Configuration	Free nucleons	Renormalized	Semiempirical
	g factors $g_I=1$ $g_s=5.586$	g factors $g_I=1.1$ $g_s=5$	g factors $g_I=1.1$ $g_s=0.7g_{\text{free}}=3.91$
$p_{1/2}$	-0.529	-0.200	0.163
$p_{3/2}$	2.529	2.400	2.037
$f_{5/2}$	0.026	0.257	0.475

IV. DISCUSSION

A. The single particle model

It is useful for orientation purposes to compute the g factors in the single particle model, even though this picture is not expected to apply for the complex Ag isotopes.

Table V lists the Schmidt values of g for $p_{1/2}$, $p_{3/2}$, and $f_{5/2}$ orbits for different choices of g_I and g_s : free nucleon values, the renormalized values which give reasonable results for the $\frac{1}{2}^-$ ground state g factor, and the more universal values which are now widely used for a large series of nuclei. It is interesting to note that, with plausible choices of g_s , the measured values of the g factor of the $\frac{1}{2}^-$ ground state and of the $\frac{5}{2}_1^-$ state can be reproduced by the calculation. The single particle prediction for the $\frac{3}{2}_1^-$ state is, however, always too large.

B. Weak coupling model

The structure of the $^{107,109}\text{Ag}$ isotopes has traditionally been analyzed in the framework of the weak coupling of

an odd particle to an even-even core.⁴ De Shalit considered the case where the angular momentum of the valence single particle nucleon is $j = \frac{1}{2}$. The coupling to a core with $I_c=2$ leads to a "doublet" with $I = \frac{3}{2}$ and $I = \frac{5}{2}$, while coupling to the ground state $I_c=0$, yields $I = \frac{1}{2}$. In particular for the Ag isotopes, a $p_{1/2}$ proton is coupled to the $^{106,108}\text{Pd}$ cores; alternatively, a $p_{1/2}$ proton hole can be coupled to $^{108,110}\text{Cd}$ cores. The g factor of a state of spin I in the odd nucleus is given by

$$g_I = \frac{g_j}{2} \left| 1 + \frac{j(j+1) - I_c(I_c+1)}{I(I+1)} \right| + \frac{g_c}{2} \left| 1 + \frac{j(j+1) - I_c(I_c+1)}{I(I+1)} \right|,$$

where g_j is taken as the g factor of the $\frac{1}{2}^-$ ground state of the $^{107,109}\text{Ag}$ nuclei, and the subscript c refers to the core. The results of this calculation are shown in Table VI and in Fig. 4.

While the ratios of g factors agree reasonably well with the model, the experimental moments are larger than the

TABLE VI. Comparison of experimental g factors and their ratios with model predictions.

Expt. ^a	Weak coupling ^b		IBA ^c	Symmetric rotor $\gamma=0^d$			Asymmetric rotor ^e		
	$p_{1/2} + \text{Pd}$	$p_{1/2} + \text{Cd}$		$K = \frac{1}{2}$	$\eta=3.2$ $K = \frac{3}{2}$	$K = \frac{1}{2}, \frac{3}{2}$	$\gamma=20^\circ$	$\gamma=24^\circ$	
^{107}Ag									
$g_{1/2}$	-0.227		-0.229	-0.22	-0.22	-0.22	-0.10	-0.12	
$g_{3/2}$	0.61(12)	0.52(3)	0.45(12)	0.522	0.14	1.43	0.12	0.55	0.83
$g_{5/2}$	0.41(7)	0.27(1)	0.23(5)	0.553	0.38	0.83	0.36	0.45	0.38
$g(\frac{3}{2})$									
$g(\frac{5}{2})$	1.5(2)	1.92(13)	1.96(67)	0.944	0.37	1.72	0.33	1.25	2.19
^{109}Ag									
$g_{1/2}$	-0.261		-0.269	-0.22	-0.22	-0.22	-0.10	-0.12	
$g_{3/2}$	0.66(10)	0.48(5)	0.40(10)	0.631	0.14	1.43	0.12	0.55	0.83
$g_{5/2}$	0.29(6)	0.24(2)	0.18(3)	0.287	0.38	0.83	0.36	0.45	0.38
$g(\frac{3}{2})$									
$g(\frac{5}{2})$	2.1(3)	2.00(27)	2.22(67)	2.19	0.37	1.72	0.33	1.25	2.19

^a The g factors are taken from this work, while the g -factor ratios are averages of the data from this work and Refs. 8 and 9.

^b Calculated assuming the magnetic moments of the Pd and Cd isotopes given in Table I.

^c Reference 27.

^d $\eta=3.2$ corresponds to the deformation of the $^{106}\text{Pd } 2^+$ state. The calculation is carried out for either $K = \frac{1}{2}$, $K = \frac{3}{2}$ or Coriolis mixed $K = \frac{1}{2}$ and $K = \frac{3}{2}$ bands, and is independent of the number of neutrons.

^e These calculations were carried out without consideration of the possible effect of the different neutron numbers in ^{107}Ag and ^{109}Ag , and for $g_s=0.7g_{\text{free}}$, $\epsilon=0.26$, and $g_R=0.43$.

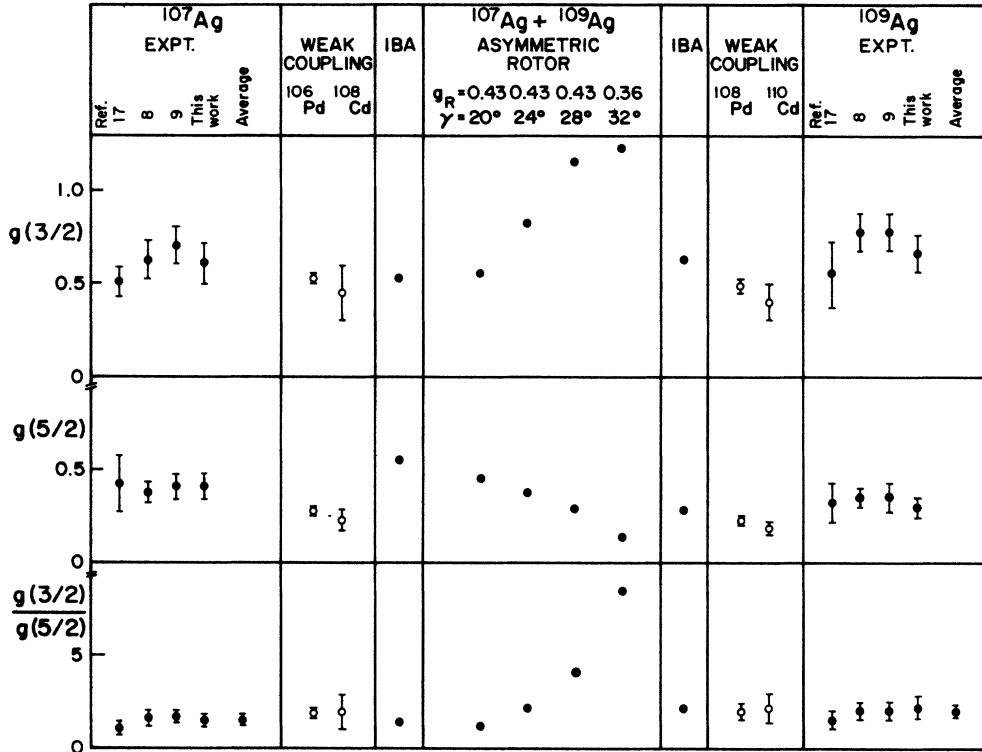


FIG. 4. Comparison of the measured g factors with some of the theoretical predictions.

model predicts. Furthermore, the formula can be rewritten as

$$g_c = [g(\frac{3}{2}) + g(\frac{5}{2})] / 2$$

from which $g_c = 0.55(6)$ and $0.51(6)$ are obtained for the ^{106}Pd and ^{108}Pd cores, respectively. This result disagrees with the measured $g(2^+)$ (Table I) but is in accord with Bohr and Mottelson's observation²² that the values of g_R are systematically larger for odd proton nuclei than for the neighboring even-even nuclei.

Note that the single particle g factor for the $\frac{5}{2}_1^-$ state ($g = 0.257$ for $g_s = 5$) is very close to that obtained from the weak coupling wave function $[p_{1/2}, 2^+]$. If the two g factors were exactly the same, one could construct a wave function

$$\psi(\frac{5}{2}) = \sqrt{(1-\alpha^2)} [p_{1/2}, 2^+]^{5/2} + \alpha f_{5/2}$$

which would yield a g factor independent of α . Thus, one would not be able to determine from the g factor alone whether the state is described by a single proton (or hole) configuration, a weak coupling scheme, or a mixture of both.

C. Axial Nilsson model

In an alternative approach, the deformed Nilsson model in which the $I^\pi = \frac{1}{2}_1^-, \frac{3}{2}_1^-, \frac{5}{2}_1^-,$ and $\frac{7}{2}_1^-$ states are members of a $K = \frac{1}{2}$ band while the $\frac{3}{2}_2^-$ and $\frac{5}{2}_2^-$ states are associated with a $K = \frac{3}{2}$ band can be invoked. It is not reasonable to assume that the $\frac{3}{2}_1^-$ and $\frac{5}{2}_1^-$ states are members of a pure $K = \frac{3}{2}$ band, because this configura-

tion would imply a $\frac{7}{2}_1^-$ state at 0.55 MeV, while the first $\frac{7}{2}_1^-$ state lies at 0.91 MeV. Nevertheless, a small admixture of $K = \frac{3}{2}$ into the basic $K = \frac{1}{2}$ band is possible via the Coriolis interaction.

The fact that the spectra of the nearby Pd nuclei are identified as vibrational is somewhat disconcerting for this deformation model. The vibrational model in its simpler form would predict a vanishing quadrupole moment for the 2_1^+ states of these nuclei, while in fact the measured quadrupole moments are appreciable (Table I). For example, for ^{108}Pd , a deformation parameter $\beta = 0.16$ is obtained from the measured spectroscopic quadrupole moment $Q(2_1^+)$ and the expression for the intrinsic quadrupole moment:

$$Q_0 = -(\frac{7}{2})Q = (3/\sqrt{5\pi})ZR_0^2\beta[1 + (\frac{4}{7})\sqrt{5/4\pi}\beta].$$

This deformation suggests a prolate shape and a wave function for the 2_1^+ states of Pd that is intermediate between vibrational and rotational descriptions.

The quadrupole moments of the $\frac{3}{2}_1^-$ and $\frac{5}{2}_1^-$ states of ^{109}Ag have also been measured by Coulomb excitation with ^4He and ^{16}O projectiles (Table I). While the magnitude of the results depends on the unknown relative signs of the matrix elements coupling neighboring $\frac{3}{2}_1^-$ or $\frac{5}{2}_1^-$ levels, it is clear that both states have *negative* quadrupole moments and, furthermore, that the $\frac{3}{2}_1^-$ state has apparently a fairly large quadrupole moment. It can be seen from the rotational model expression

$$Q(I) = Q_0[3K^2 - I(I+1)] / [(I+1)(2I+3)]$$

that if the $\frac{1}{2}^-$, $\frac{3}{2}^-$, and $\frac{5}{2}^-$ states are members of the $K = \frac{1}{2}$ band, the measured negative quadrupole moments correspond to a prolate deformation.

The Nilsson model in its simpler form was therefore applied to the odd Ag isotopes and the values of the g factors were obtained for the $\frac{1}{2}^-$, $\frac{3}{2}^-$, and $\frac{5}{2}^-$ states. The renormalized g factors were used as input parameters because they yield a good fit to the ground state moment. The free nucleon values, on the other hand, yield a g factor for the ground state a factor of 2 larger than the experimental value.

The odd proton occupies the No. 26, $K = \frac{1}{2}$, Nilsson orbit, which in the limit of zero deformation, becomes a $p_{1/2}$ state. The resulting g factors are shown in Fig. 5 as a function of the Nilsson deformation parameter $\eta = 20\beta$. In fact, as the deformation increases, the moments for neither the oblate nor the prolate shapes agree with experiment. Indeed an examination of Fig. 5 indicates that the best agreement with the measured data is obtained for $\eta = 0$, while the calculation for the prolate deformation $\eta = 3.2$ which corresponds to the quadrupole moments of the $^{106,108}\text{Pd}$ and $^{108,110}\text{Cd}$ 2_1^+ states, is in complete disagreement with experiment (Table VI).

An intriguing result has emerged from this calculation. In the limit of zero deformation, the expressions for g factors given by the Nilsson model for the $\frac{3}{2}^-$ and $\frac{5}{2}^-$ states become identical with the expression derived in the weak coupling model. Furthermore, $g(\frac{1}{2}^-)$ goes into the Schmidt value.

A calculation including Coriolis mixing was also performed in which the closest $K = \frac{3}{2}$ band (No. 19), was admixed perturbatively into the basic $K = \frac{1}{2}$ band (No. 26). A separation of 0.4 MeV between the two bands was assumed and admixtures of about 0.25% of $K = \frac{3}{2}$ into the basic $K = \frac{1}{2}$ state were obtained for a wide range of defor-

mations. The results are also shown in Fig. 5. The overall picture does not change very much, and the prolate deformation still does not represent reality.

While most of the available evidence, such as the quadrupole moments of the $\frac{3}{2}^-$ and $\frac{5}{2}^-$ states, of the $^{106,108}\text{Pd}$ and $^{108,110}\text{Cd}$ 2_1^+ states and the systematics of energy levels points to a prolate deformation, within the limitations of the axial Nilsson model, the large magnetic moment of the $\frac{3}{2}^-$ state tends to support an oblate shape. In order to understand this point, it was assumed that the two $\frac{3}{2}^-$ states seen in the Ag spectra and belonging, respectively, to the $K = \frac{1}{2}$ and $K = \frac{3}{2}$ bands, are strongly mixed. The resulting wave function can be written as

$$\psi(J = \frac{3}{2}) = \sqrt{1 - \alpha^2} \psi(K = \frac{1}{2}) + \alpha \psi(K = \frac{3}{2}).$$

The g factor of the state becomes a strong function of α , and, for example, $g(\frac{3}{2}^-) = 0.135, 0.633, \text{ and } 0.745$ for $\alpha = 0, -0.25, \text{ and } -0.3$, respectively. Thus a 9% mixing of $K = \frac{3}{2}$ into the basic $K = \frac{1}{2}$ state is needed to change the magnetic moment sufficiently to agree with experiment while the Coriolis mixing calculation yields a value of α which is much too small ($\alpha \sim 0.05$).

D. Triaxial Nilsson plus rotor model

A calculation of properties of the Ag isotopes has been carried out in the asymmetric rotor model by Vieu *et al.*²³ The Hamiltonian is written as

$$H = H_c + H(\text{Nilsson}) + H(\text{pairing}),$$

where

$$H_c = \Sigma \hbar^2 R_K^2 / [8\beta \epsilon^2 \sin^2(\gamma + 2k\pi/3)].$$

An additional parameter γ and a new source of K mixing ($\Delta K = 2$) over and above that given by the Coriolis interaction ($\Delta K = 1$) is introduced. Further details are given in Ref. 23. The authors obtained ϵ and γ from a fit to the energy levels, but did not include in this fit the static properties of the $\frac{3}{2}^-$ and $\frac{5}{2}^-$ states, namely the quadrupole and magnetic moments. Their best fit yields $\epsilon = 0.26$ and $\gamma = 32^\circ$. The axial asymmetry is large and slightly on the oblate side. This choice of ϵ and γ , however, leads to static properties that do not agree well with experiments; for example, the signs of the predicted quadrupole moments $Q(\frac{1}{2}^-) = 0.2904$ and $Q(\frac{5}{2}^-) = 0.2281$ are opposite to those of the measured moments. The calculated g factors (Table VII) are not dissimilar to the values obtained with the symmetric Nilsson model for an oblate shape $\eta = -2$ (Fig. 5), but do not agree with experiment either.

Better results for the static properties are obtained in the asymmetric rotor model if the parameter γ is made smaller than 30° , corresponding to a more prolate shape. Calculations have been carried for several sets of parameters and some of the results are listed in Table VII. The parameter ϵ has been kept fixed at the value $\epsilon = +0.26$, but γ has been varied from 20° to 32° . The reduction in γ not only changes the sign of the quadrupole moments but

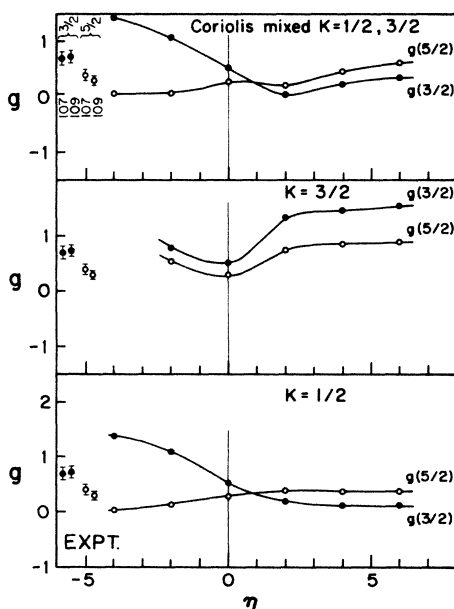


FIG. 5. Deformation dependence of the g factors in the symmetric rotor model.

TABLE VII. Static moments in the particle asymmetric rotor model for Ag calculated for a deformation parameter $\epsilon=0.26$ and the semiempirical g factor $g_s=0.7g_{\text{free}}$.

g, Q	g_R	0.43	0.43	0.43	0.36
	γ	20°	24°	28°	32°
$g(\frac{1}{2})$		-0.10	-0.12	-0.14	-0.18
$g(\frac{3}{2})$		0.55	0.83	1.15	1.23
$g(\frac{5}{2})$		0.45	0.38	0.28	0.14
$g(\frac{3}{2})$		1.25	2.19	4.11	8.48
$g(\frac{5}{2})$					
$Q(\frac{3}{2})$ eb		-0.46	-0.24	0.07	0.29
$Q(\frac{5}{2})$ eb		-0.75	-0.59	-0.28	0.23

also produces magnetic moments in fairly good agreement with experiment (Table VII). On the other hand, increasing the spin quenching from $g_s=0.7g_{\text{free}}$ to $g_s=0.6g_{\text{free}}$ reverses the sign of the ground state magnetic moment. While the resulting quadrupole moments now have the correct sign, their magnitude and ratio [$Q(\frac{5}{2}^-)/Q(\frac{3}{2}^-) < 1$] do not yet fit experiment. It would certainly be worthwhile to actually measure the signs of the relevant matrix elements in order to obtain a unique solution for the experimental quadrupole moments. The optimum fit requires a γ in the range $20^\circ < \gamma < 24^\circ$, but even in this narrow range, the results are still very sensitive to the choice of γ and g_s . The present data and analysis are supported by recent measurements²⁴ of the magnetic moment of the 1.734 MeV isomeric state in ^{105}Ag . This particular measurement together with similar data from $^{104,105}\text{Pd}$ and $^{104,107}\text{Ag}$ have been interpreted by means of the cranked shell model and the assumption of a configuration-dependent triaxiality that reflects the interaction of a soft nuclear core with the quasiparticle.

E. Interacting boson approximation calculation

The properties of the low lying levels of the Ag isotopes have been thoroughly analyzed in terms of an interacting Bose-Fermi model by Wood *et al.*²⁵ They have obtained fairly reasonable agreement with the experimental data (Table VI). They show that while these calculations can easily fit energy spectra, additional data such as $B(M1)$'s, $B(E2)$'s, and magnetic moments are required to critically test the model in agreement with the recent conclusions of Loiselet *et al.*¹² reached from a measurement of the lifetimes of the $\frac{5}{2}_1^-$ and $\frac{9}{2}_1^-$ states of $^{107,109}\text{Ag}$.

V. CONCLUSION

The magnetic moments of the $\frac{3}{2}_1^-$ and $\frac{5}{2}_1^-$ states of the Ag isotopes have been measured by the transient hyperfine magnetic field technique. The ratios of these moments are independent of the details of the transient field and are therefore free of systematic errors arising from the incomplete understanding of the field. The absolute values of the measured g factors have uncertainties of about 15% which arise mostly from uncertainties in the calibration of the transient field.

Both the ratios and absolute values of the magnetic moments agree qualitatively with either weak coupling or IBFM models. A calculation done with Nilsson deformed nucleus wave functions provides the best results for the limit of zero deformation (which was shown to be identical to the weak coupling scheme), a conclusion somewhat at odds with the collective character of the 2_1^+ states of the even-even cores in $^{106,108}\text{Pd}$ and $^{108,110}\text{Cd}$ and with the observation of large quadrupole moments for the $\frac{3}{2}_1^-$ and $\frac{5}{2}_1^-$ states in ^{109}Ag .

This puzzle is to a large extent solved by giving up axial symmetry, as was done by Vieu *et al.*²³ in their particle-asymmetric rotor model. It has been shown here that the static magnetic dipole and electric quadrupole moments of the excited $\frac{3}{2}_1^-$ and $\frac{5}{2}_1^-$ states are extremely sensitive to the choice of the deformation parameters ϵ and γ . The original choice²³ ($\epsilon=+0.26$, $\gamma=32^\circ$) which gave the best fit to energy levels and transition rates, yields quadrupole moments with the wrong sign, and a value of $g(\frac{3}{2}^-)$ which is much too large. A change towards prolate deformation ($\epsilon=0.26$, $\gamma=20^\circ-24^\circ$) produced quadrupole moments of the right sign, improved the g factors, gave an acceptable energy spectrum, and resulted in even better values of $B(M1)$'s and $B(E2)$'s than obtained with the earlier choice of parameters. The fits to the g factors are not yet perfect, indicating that these nuclei may exhibit greater complexity than is afforded by the asymmetric rotor model. The data and calculations presented here demonstrate that the static properties of excited states constitute an essential input into the phenomenological determination of the asymmetry parameter γ and effective nucleon g factors and provide stringent and challenging tests for theory.

ACKNOWLEDGMENTS

We thank Dr. H. Jaqaman for performing Hartree-Fock calculations with the Skyrme interactions which yield prolate minima for ^{108}Pd and ^{109}Ag and Mr. R. Klein for his careful target preparation. The work carried out at Rutgers University was partially supported by the National Science Foundation, while G. A. Leander was partly supported by the U.S. Department of Energy under Contract No. DE-AC05-76OR00033.

*Present address: Memorial-Sloan Kettering Cancer Center, 1275 York Ave., New York, NY 10021.

†Present address: Indigo, R&R, Kyriat Weizmann, P.O. Box 150, Rehovot 76101, Israel.

‡Present address: EMR, Princeton, NJ 08540.

¹N. K. B. Shu, R. Levy, N. Tsoupas, A. Lopez-Garcia, W. Andrejscheff, and N. Benczer-Koller, Phys. Rev. C **24**, 954 (1981).

- ²M. Sambataro and A. E. L. Dieperink, *Phys. Lett.* **107B**, 249 (1981).
- ³O. Scholten, Ph.D. thesis, University of Groningen, 1979; F. Iacchello and O. Scholten, *Phys. Rev. Lett.* **43**, 679 (1979).
- ⁴A. de Shalit, *Phys. Rev.* **122**, 1530 (1961).
- ⁵V. Paar, *Nucl. Phys.* **A211**, 29 (1973).
- ⁶A. W. Kuhfeld and N. M. Hintz, *Nucl. Phys.* **A247**, 152 (1975).
- ⁷L. Hasselgren, C. Fahlander, F. Falk, L. O. Edvardson, J. E. Thun, B. S. Ghuman, and B. Skaali, *Nucl. Phys.* **A264**, 341 (1976).
- ⁸A. E. Stuchbery, L. D. Wood, R. A. Bark, and H. H. Bolotin, *Hyp. Int.* **20**, 119 (1984).
- ⁹D. Bazzacco, F. Brandolini, P. Pavan, C. Rossi-Alvarez, R. Zannoni, and M. DePoli, *Nuovo Cimento* **84**, 106 (1984).
- ¹⁰T. R. Miller and M. Takeda, *Nucl. Phys.* **A221**, 392 (1974).
- ¹¹B. Harmatz, *Nucl. Data Sheets* **34**, 643 (1981).
- ¹²M. Loiselet, R. Holzmann, M. A. Van Hove, and J. Vervier (unpublished).
- ¹³B. Harmatz, *Nucl. Data Sheets* **30**, 305 (1980).
- ¹⁴R. L. Haese, F. E. Bertrand, B. Harmatz, and H. J. Martin, *Nucl. Data Sheets* **37**, 289 (1982).
- ¹⁵P. de Gelder, E. Jacobs, and D. de Frenne, *Nucl. Data Sheets* **38**, 545 (1983).
- ¹⁶J. M. Brennan, M. Hass, N. K. B. Shu, and N. Benczer-Koller, *Phys. Rev. C* **21**, 574 (1980).
- ¹⁷T. R. Miller, P. D. Bond, W. A. Little, S. M. Lazarus, M. Takeda, G. D. Sprouse, and S. S. Hanna, *J. Phys. Soc. Jpn.* **34**, 107 (1973).
- ¹⁸K. Johansson, E. Karlsson, L. O. Norlin, R. A. Windahl, and M. R. Ahmed, *Nucl. Phys.* **A188**, 600 (1972); V. Singh, *J. Phys. Soc. Jpn.* **29**, 1111 (1970).
- ¹⁹M. J. Throop, I. Hall, I. M. Naqib, D. J. Thomas, and B. Wakefield, *Phys. Lett.* **41B**, 585 (1972).
- ²⁰R. P. Harper, A. Christy, I. Hall, I. M. Naqib, and B. Wakefield, *Nucl. Phys.* **A162**, 162 (1971); W. R. Lutz, J. A. Thomson, R. P. Scharenberg, and R. D. Larsen, *Phys. Rev. C* **6**, 1385 (1972).
- ²¹N. K. B. Shu, D. Melnik, J. M. Brennan, W. Semmler, and N. Benczer-Koller, *Phys. Rev. C* **21**, 1828 (1980).
- ²²A. Bohr and B. Mottelson, *Nuclear Structure* (Benjamin, New York, 1975), Vol. II, p. 305, tables 5–14.
- ²³Ch. L. Vieu, S. E. Larsson, G. Leander, and I. Ragnarsson, *Phys. Rev. C* **22**, 853 (1980).
- ²⁴H. J. Keller, S. Frauendorf, U. Hagemann, L. Kaubler, H. Prade, and F. Stary, *Nucl. Phys.* **A444**, 261 (1985).
- ²⁵L. D. Wood, H. H. Bolotin, I. Morrison, R. A. Bark, H. Yamada, and A. E. Stuchbery, *Nucl. Phys.* **A427**, 639 (1984).